2011 American Control Conference
on O'Farrell Street, San Francisco, CA, USA
June 29 - July 01, 2011

Detecting and analyzing non-linear effects in respiratory impedance measurements

Clara Ionescu, Johan Schoukens and Robin De Keyser

Abstract— **This article describes the nonlinear effects in the respiratory impedance and in the related measurement instrumentation during the forced oscillation technique (FOT) measurements. First, the principle of FOT-measurements and nonlinear variance analysis is explained. Two methods are considered to detect nonlinear effects: a robust method and a fast method. These methods are employed to compare the nonlinear distortions in a prototype device and a commercial device, respectively. The identification signal for the respiratory impedance is optimized to reduce the nonlinear distortions. Finally, the nonlinear effects are measured in the respiratory impedance. A set of lung function tests are performed in several groups of patients with various lung conditions (healthy, asthma, cystic fibrosis, smoking). Based on the measured data from the patients, the corresponding nonlinear distortions can be quantified and evaluated for classification purposes.**

I. Introduction

The frequency response function of the respiratory impedance has been extensively studied over the last decades. New technologies for data processing and new methods for analysis, diagnosis and simulation of the human respiratory system have contributed to the progress in this field [3], [6], [9], [11]. An increase in interest has occurred for the low frequency behaviour of the respiratory impedance [1], [10]. This can be measured with non-invasive tests, such as the forced oscillation technique, based on superposition of a multisine signal onto the normal (i.e. unforced) breathing of the subject [11].

There is evidence that when measuring the respiratory impedance, the lung function testing device imposes a load at the mouth of the patient [2]. This, in turn, introduces nonlinear distortions originating from the device itself [5]. Apart from these, additional nonlinear effects may come from the biological tissue. The dynamic response of the lungs to the testing protocol is assumed to be linear, but this does not mean that in the measurement data only linear effects are captured.

Little is known about the effects of nonlinearities in the values of the respiratory impedance [4], [5]. The respiratory system and the related measurement instrumentation are considered to be linear, a condition which enables a set of simplifying assumptions to obtain equivalent electrical models [11]. However, in practice it is not possible to ensure linearity and often one is not even aware of the presence of these nonlinear distortions. The question arises to what extent these nonlinearities affect the obtained results and if these are still reliable. This leads to the points that are addressed in this article. *Firstly*, we would like to know to what extent is the measurement instrumentation for the respiratory impedance affected by nonlinear distortions. In other words, to detect if the measurement of the respiratory impedance is affected by the nonlinear distortions in the measurement instrumentation and if so, to correct for these effect in the end result. *Secondly*, we explore the possibility to detect, qualify and quantify the presence of nonlinear distortions in relation to the state of the respiratory system with disease.

The work presented in this paper aims to provide a first proof of concept that nonlinear effects are present in the respiratory impedance and they can vary from one group of subjects to another (i.e. with pathology). As such, altering the lung parenchyma will introduce asymmetry of flow circulation and non-uniform diffusion, leading to variations in the flow-pressure relation which are then used to characterize the parameters of the respiratory system. We investigate the separate effects of nonlinear distortions from the measuring device itself; followed by an analysis of nonlinear effects in asthma, cystic fibrosis, smoking and healthy subjects. The results show that the proposed signal processing technique is able to detect nonlinear effects with significant variations between different pathologies versus the healthy case.

The present article is organized as follows. The second section describes the subjects we used to gather the measurements for the respiratory impedance and the methods used to process the signals and detect the nonlinear contributions. Both nonlinear contributions from the device as well as from the patient are presented. The results are given and discussed in the third and fourth sections, respectively. A conclusion section summarizes the main outcome of this investigation and points towards future steps in this research line.

II. Materials and methods

A. Forced oscillation technique (FOT)

The standard (commercialized) forced oscillation technique is a non-invasive technique which applies small air pressure oscillations to the respiratory system of a subject who is breathing spontaneously [11].

The pressure oscillations are generated by means of a loudspeaker LS connected to a chamber, as in Figure 1.

This work was financially supported solely by UGent-EeSA department.

C. Ionescu and R. De Keyser are with the Faculty of Engineering, EeSA-Department of Electrical energy, Systems and Automation, Universiteit Gent, Technologiepark 913, 9052 Gent-Zwijnaarde, Belgium ClaraMihaela.Ionescu@UGent.be Robain.DeKeyser@UGent.be

J. Schoukens is with the Faculty of Engineering, Department of Fundamental Electricity and Instrumentation, Vrije Universiteit Brussel, Building K - Room K430, Pleinlaan 2, 1050 Brussels, Belgium Johan.Schoukens@vub.ac.be

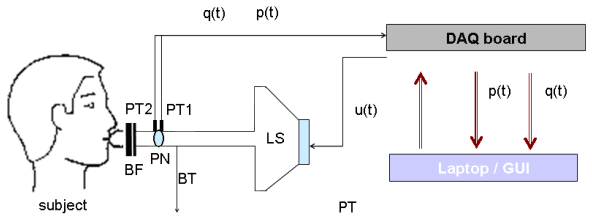

Fig. 1. FOT-device: $u(t)$ = input signal, $q(t)$ = air flow at mouth, $p(t)$ = air pressure at mouth, LS = loudspeaker, BT = bias tube, PT = pressure sensor, PN = pneumotachograph, BF = biological filter.

The loudspeaker is driven by a power amplifier fed with the oscillating signal $u(t)$ generated by a computer. The movement of the loudspeaker cone generates a pressure oscillation inside the chamber, which is applied to the patient's respiratory system by means of a tube connecting the loudspeaker chamber and an anti-bacterial filter BF. The bias tube BT allows the patient to breath fresh air during the measurements. Pressure $p(t)$ and flow $q(t)$ are measured at the mouthpiece with the combination of two pressure sensors PT and a pneumotachograph PN. The excitation pressure signal is kept within a range of a peak-to-peak size of $0.1 - 0.3\,\mathrm{kPa}$, typically for patient safety, comfort and to ensure linearity. In this study, we consider the same peak-to-peak range for applying multisine oscillations in the frequency range: $0.5 - 21.9\,\mathrm{Hz}$. Using well-designed multisines, is possible to reduce the impact of the nonlinear distortions on the impedance measurements. Briefly, it has been shown that a multisine with only odd excited harmonics provides a better estimate than other types of signals [12].

One of the most common non-parametric representations of the impedance Z_r (kPa s/l) is obtained assuming a linear dependence between the breathing and superimposed oscillations at the mouth of the patient [3]. Using the electrical analogy in which pressure corresponds to voltage and flow corresponds to current, the respiratory impedance Z_r can be obtained from the spectral (frequency domain) ratio:

$$Z_r(j\omega) = \frac{S_{PU(j\omega)}}{S_{QU(j\omega)}} \tag{1}$$

where $S(j\omega)$ denotes the cross-correlation spectra between the various input-output signals, $\omega\,\mathrm{rad/s}$ is the angular frequency and $j = \sqrt{-1}$, resulting in a complex variable evaluated in each frequency point of interest [8]. The frequency where the imaginary part of the impedance crosses zero is called the *resonance frequency* and it depends on the balance between the different kind of mechanical properties (elastic, inertial). This then allows clinicians to visually classify between healthy and pathologic cases, e.g. the resonance frequency changes significantly from $7 - 9\,\mathrm{Hz}$ for a healthy adult, to $6 - 20\,\mathrm{Hz}$ for a COPD patient.

A novel (prototype) device was designed for a lower frequency range than the standard FOT device. The standard FOT applies oscillations from 4-48 Hz. Lower frequencies hold valuable information from medical point of view, since they are closer to the breathing signal and thus give valuable information about the respiratory mechanics in the frequency range of the breathing $(0.1 - 0.3\,\mathrm{Hz})$. In Figure 2, the respiratory impedance of a patient, by means of its real (resistance) and imaginary (reactance) parts, is obtained with both a prototype and a commercial device. The results look nearly the same, although the results with the prototype appear to be slightly noisier. Hence, we may conclude that the prototype can be reliably used for the standard frequency range. Additionally, we shall make use of this prototype to assess respiratory impedance at frequencies below 4 Hz.

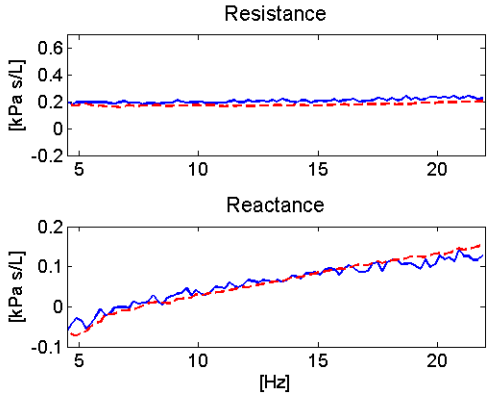

Fig. 2. Respiratory impedance for a healthy subject obtained with FOT. Blue solid line: prototype device; red dotted line: commercial device.

B. Subjects and Patients

The nonlinear analysis is performed on three test groups. In the first group, the nonlinear effects in the respiratory impedance of children aged $8 - 17\,\mathrm{years}$ with cystic fibrosis are compared to the results for healthy children aged $9 - 11\,\mathrm{years}$. Cystic fibrosis is a genetic disorder where excess mucus can be produced in the lungs, thus clogging the airways [7]. In the second group, the nonlinear effects in the respiratory impedance of children aged $8 - 17\,\mathrm{years}$ with asthma are compared to the results for same healthy children. Asthma is a predisposition to chronic inflammation of the lungs in which the airways are reversibly narrowed [7]. In a third group, the nonlinear effects in the respiratory impedance of smokers and non-smokers aged $23 - 25\,\mathrm{years}$ are compared. The smokers were instructed to smoke a cigarette before the measurements.

C. Identification of the nonlinear contributions

The fundamental difference between a linear time invariant system and a nonlinear system is that the nonlinear system transfers energy from one frequency in the input signal to other frequencies in the output signal.

The influence of nonlinear distortions on the frequency response function measurements are determined by using a random phase multisine:

$$U(t) = \sum_{k=1}^{N} A_k \cos(k\omega_0 t + \phi_k) \tag{2}$$

as an input signal, with A_k the amplitude different from zero only for the odd k values, $\omega_0 = 2\pi f_0$ and $f_0 = 0.1$ Hz, ϕ_k the phase uniformly and independently distributed in the $[0; 2\pi]$ interval and N the number of sinusoids.

The best linear approximation (BLA) of a nonlinear system can be viewed as a minimization of the mean squared error between the true output of the nonlinear system and the output of a linear model. The estimated BLA $\hat{G}_{BLA}(j\omega_k)$ of a wide class of nonlinear systems, obtained using a random phase multisine, can be written as:

$$\hat{G}_{BLA}(j\omega_k) = G_{BLA}(j\omega_k) + G_S(j\omega_k) + N_G(j\omega_k) \quad (3)$$

with $G_{BLA}(j\omega_k)$ the true best linear approximation (BLA) of the nonlinear system, $G_S(j\omega_k)$ the zero mean stochastic nonlinear contributions and $N_G(j\omega_k)$ the measurement noise [12]. The stochastic nonlinear contributions $G_S(j\omega_k)$ can be extracted by averaging from a manifold of experiments M containing different phase realizations in the excitation signal from (2). The measurement noise $N_G(j\omega_k)$ can be minimized by measuring longer, thus by increasing N.

In Figure 3, one can easily understand the underpinning principle of detecting these nonlinearities. The acquired information can be done in one, or more realizations (experiments). Each time that a new realization M is made, another random phase multisine with P periods of N samples is send to the system under observation, hence providing extra information.

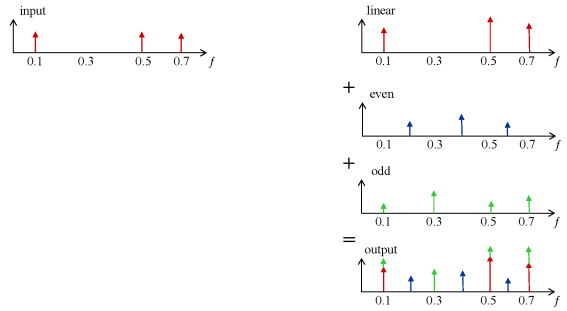

Fig. 3. A schematic representation of the input-output contributions.

Figure 4 depicts a schematic of the input and output measurements corrupted by noise and the corresponding BLA. In [13], a variance analysis procedure has been proposed that allows to detect and quantify the stochastic nonlinear distortions $G_S(j\omega_k)$ and the disturbing noise $N_G(j\omega_k)$. Two measurement methods can be applied:

- a robust method, which uses different random phase realizations of an odd multisine excitation to get information about the stochastic nonlinear distortions;
- a fast method, which uses only one realization of an odd random phase multisine with random harmonic grid.

The information about the stochastic nonlinear distortions is obtained via the detection lines (non-excited harmonics) in the output DFT spectrum. To compensate for spectral impurity of the input, a first order correction is applied

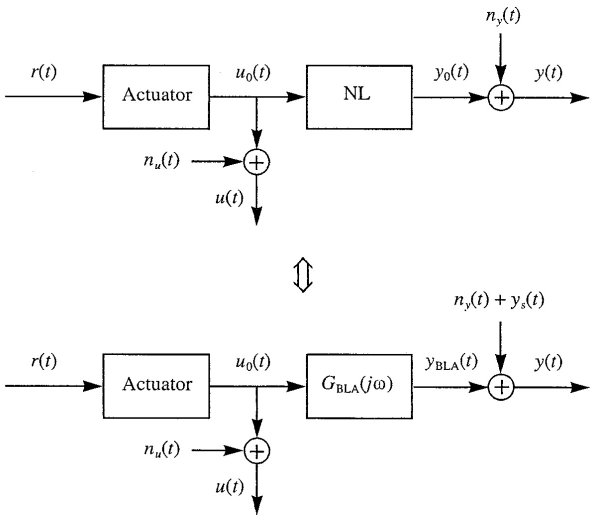

Fig. 4. Input $u(t)$ and output $y(t)$ measurements with noise from a nonlinear system driven by an actuator with input signal $r(t)$ (top), and its corresponding best linear approximation (under).

to the output DFT spectrum. The use of an odd random phase multisine with a random harmonic grid provides also a classification of the nonlinear distortions in even and odd contributions in the corrected output DFT spectrum.

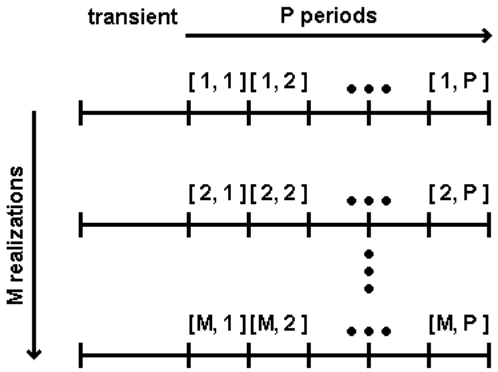

Fig. 5. Measurement procedure for the robust method: P periods of length N measured from the steady state response with an odd multisine input. The experiment is then repeated M times, each time with a different odd random phase multisine realization.

Figure 5 shows the principle of measuring the BLA using the robust method, i.e. by averaging between M realizations with P periods. If the input signal is known and uncorrupted with noise, one can obtain the non-parametric estimation of the BLA as $G_{BLA}(j\omega_k)$, the variance of the stochastic nonlinear distortions $var(G_S(j\omega_k))$ and the variance of the noise $\sigma_{GBLA,n}$. Given that $n_y(t)$ is a stochastic signal and $y_s(t)$ a periodic signal depending on the phase realization of the input (reference) signal $r(t)$, the frequency response function of the m^{th} realization and p period, $G^{[m,p]}(j\omega_k)$ can be written as:

$$G^{[m,p]}(j\omega_k) = G_{BLA}(j\omega_k) + \frac{Y_S^{[m]}(k)}{U_0^{[m]}(k)} + \frac{N_Y^{[m,p]}(k)}{U_0^{[m]}(k)} \quad (4)$$

where $X^{[m,p]}(k)$ is the discrete Fourier transform spectrum of the p^{th} period of the m^{th} multisine realization. Next, the BLA, variance of the nonlinear distortions and noise variance can be estimated as:

$$\hat{G}^{[m]}(j\omega_k) = \frac{1}{P}\sum_{p=1}^{P} G^{[m,p]}(j\omega_k) \tag{5}$$

$$\hat{G}_{BLA}(j\omega_k) = \frac{1}{M}\sum_{m=1}^{M} \hat{G}^{[m]}(j\omega_k) \tag{6}$$

$$\hat{\sigma}^2_{\hat{G}^{[m]}}(k) = \sum_{p=1}^{P} \frac{|G^{[m,p]}(j\omega_k) - \hat{G}^{[m]}(j\omega_k)|^2}{P(P-1)} \tag{7}$$

$$\hat{\sigma}^2_{\hat{G}_{BLA}}(k) = \sum_{m=1}^{M} \frac{|G^{[m]}(j\omega_k) - \hat{G}_{BLA}(j\omega_k)|^2}{M(M-1)} \tag{8}$$

$$\hat{\sigma}^2_{\hat{G}_{BLA,n}}(k) = \frac{1}{M^2}\sum_{m=1}^{M} \hat{\sigma}^2_{\hat{G}^{[m]}}(k) \tag{9}$$

$$var(G_S(j\omega_k)) \approx M(\hat{\sigma}^2_{\hat{G}_{BLA}}(k) - \hat{\sigma}^2_{\hat{G}_{BLA,n}}(k)) \tag{10}$$

where $\hat{X}^{[m]}$ is the estimated spectrum of the m^{th} realization, $\hat{G}_{BLA}(j\omega_k)$ is the estimation of BLA, $\hat{\sigma}^2_{\hat{G}_{BLA}}(k)$ is the estimation of the total variance (stochastic nonlinear variance + noisevariance) averaged over the M experiments, $\hat{\sigma}^2_{\hat{G}_{BLA,n}}(k)$ is the variance of the noise averaged over the M experiments and $var(G_S(j\omega_k))$ is the variance of the stochastic nonlinear distortion with respect to one multisine realization. In other words, the total variance and noise variance averaged over the M experiments give an indication upon the reliability of the measured frequency response functions. The variance of the stochastic nonlinear distortion for each realization gives an indication of how much distortion is present in the system with each experiment.

The fast method is then a special case of the robust method, with $M = 1$. As such, the variance is expected to have higher values and less reliability for the fast method than in the robust method. For all the results presented in this paper, the robust method will be employed.

III. Results

A. Nonlinear effects from the measurement instrumentation

By applying the measurement methods on the FOT-device with input $u(t)$, the applied voltage to the loudspeaker, and output $q(t)$, the resulting flow and $p(t)$, the resulting pressure, one can detect the nonlinear distortion in the measurement instrumentation. Figure 6 shows the relatively big influence of noise in our prototype, which is reflected in the slightly noisier result for the respiratory impedance in Figure 2. The nonlinear distortion in the commercial device is smaller for frequencies > 15 Hz, but larger for frequencies < 6 Hz, compared to the prototype. This is the main reason for the better results of our prototype at lower frequencies.

The applied excitation signal can be optimized by making a nonlinear variance analysis. Figure 7 shows that the variance of the odd nonlinear stochastic distortion is smaller

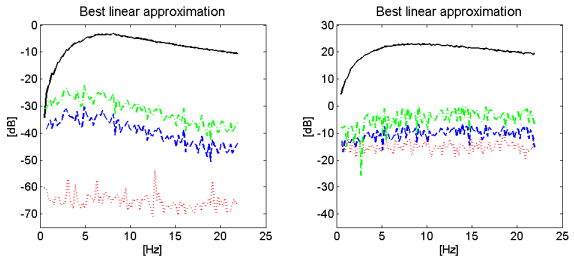

Fig. 6. Measurement of the best linear approximation (BLA) of the device impedance Z_{device} of the commercial device (left) and prototype (right) **on a calibration tub**e. Black solid line: BLA; blue dashed line: total variance (sum noise and stochastic nonlinear distortion); red dotted line: noise variance, green dash-dot line: variance of the stochastic nonlinear distortion w.r.t one multisine realisation.

when using an odd multisine excitation signal during measurements. The even nonlinearities are higher than the nonlinear contribution in the output of the odd multisine. This is mostly visible at higher frequencies, where a cumulative effect of distortions is coming from the lower excitation frequencies. By choosing an odd multisine as excitation signal, the variance of the stochastic nonlinear distortion, and consequently the total variance, is reduced with a factor three. The noise variation is unaffected by the input signal (as expected).

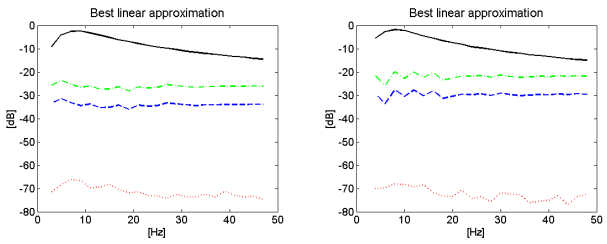

Fig. 7. Measurement of the best linear approximation (BLA) of the device impedance Z_{device} of the commercial device with odd multisine U_{odd} (left) and even multisine U_{even} (right). Black solid line: BLA; blue dashed line: total variance (sum noise and stochastic nonlinear distortion); red dotted line: noise variance, green dash-dot line: variance of the stochastic nonlinear distortion w.r.t one multisine realisation.

A better signal-to-noise ratio can be obtained by amplifying the input signal. However this generally has an effect on the nonlinear distortions in the system, e.g. through saturation of the loudspeaker or the amplifier. When the amplification of the signal is too big, the total variance of the BLA will increase through an increased variance of the stochastic nonlinear distortion. This can be observed in Figure 8, and recalling (2).

Sometimes an amplification of the lower frequencies is applied in the multisine identification signal. Consequently, this increases the nonlinear distortion at these lower frequencies and a correct interpretation of the corresponding results can be compromised. We are using the information gathered in this step of the identification process to correct for the nonlinearities coming from the device in our respiratory impedance values.

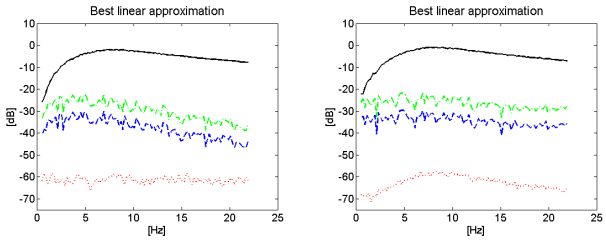

Fig. 8. Measurement of the best linear approximation (BLA) of the device impedance Z_{device} of the commercial device with $\frac{1}{2}U_{odd}$ (left) and $2U_{odd}$ (right). Black solid line: BLA; blue dashed line: total variance (sum noise and stochastic nonlinear distortion); red dotted line: noise variance, green dash-dot line: variance of the stochastic nonlinear distortion w.r.t one multisine realisation.

B. Nonlinear effects from the respiratory system

By applying the measurement methods on the respiratory impedance with input $q(t)$, the flow at the mouth, and output $p(t)$, the corresponding pressure, one can detect the nonlinear distortion in the respiratory impedance.

Figure 9 shows that for a patient with cystic fibrosis the even nonlinearities (green line) in the corrected output DFT spectrum at frequencies $< 8\,\mathrm{Hz}$ are increasing.

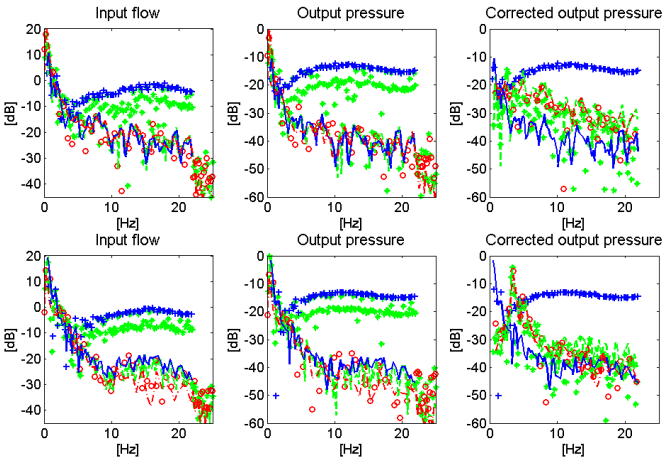

Fig. 9. Input (left column), output (middle column) and corrected DFT spectrum (right column) of a **cystic fibrosis** (top row) and a **healthy** patient (bottom row). Blue '+': excited odd harmonics; red 'o': non-excited odd harmonics; green '*': non-excited even harmonics. Blue solid line: variance of the excited odd harmonics; red dash-dot line: variance of the non-excited odd harmonics; green dashed line: variance of the non-excited even harmonics.

Figure 10 depicts the measurements performed in one asthmatic children, revealing an increase of the even and odd nonlinearities over the whole frequency range.

Finally, Figure 11 shows that the even and odd nonlinear contributions had a higher level in the corrected output DFT spectrum of a smoker subject. One may observe that the variance of the stochastic nonlinear distortions is larger in the impedance of smokers. Their corresponding BLA are given in Figure (12).

IV. Discussion

In this paper, we first quantify the nonlinear effects in a commercial FOT device and our in-house build prototype.

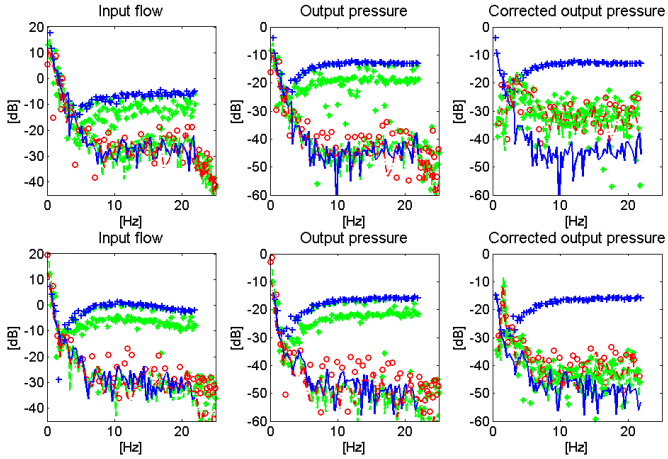

Fig. 10. Input (left column), output (middle column) and corrected DFT spectrum (right column) of an **asthma** (top row) and a **healthy** patient (bottom row). Blue '+': excited odd harmonics; red 'o': non-excited odd harmonics; green '*': non-excited even harmonics. Blue solid line: variance of the excited odd harmonics; red dash-dot line: variance of the non-excited odd harmonics; green dashed line: variance of the non-excited even harmonics.

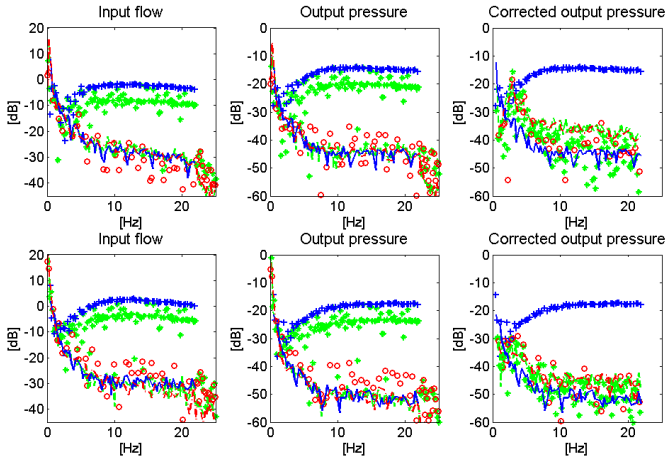

Fig. 11. Input (left column), output (middle column) and corrected DFT spectrum (right column) of a **smoker** (top row) and a **non-smoker** (bottom row). Blue '+': excited odd harmonics; red 'o': non-excited odd harmonics; green '*': non-excited even harmonics. Blue solid line: variance of the excited odd harmonics; red dash-dot line: variance of the non-excited odd harmonics; green dashed line: variance of the non-excited even harmonics.

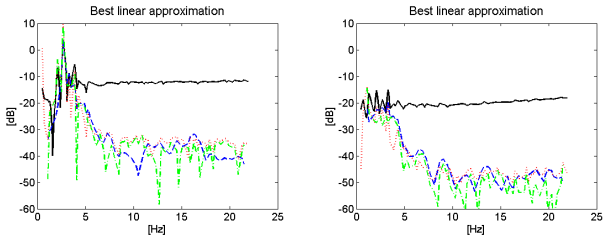

Fig. 12. Measurement of the best linear approximation (BLA) of the respiratory impedance $Z_{respiratory}$ of a smoker (left) and non-smoker (right). Black solid line: BLA; blue dashed line: total variance (sum noise and stochastic nonlinear distortion); red dotted line: noise variance, green dash-dot line: variance of the stochastic nonlinear distortion w.r.t one multisine realisation.

This implies that the results for the nonlinear effects in the respiratory impedance of different patients can only be compared with measurements made on the same FOT-device. A simple correction for these influences is suggested by relating the obtained results to the measurements on a calibration tube, as given by Figure 6.

Next, we take a look at the nonlinear distortions introduced by the respiratory system itself, by comparing results between healthy and non-healthy lungs. Apart from the values of the BLA itself, differences in the non-excited even harmonics were observed between all compared data. In Figure 9 we observed that a difference of about $10\,\mathrm{dB}$ is obtained in the non-excited even harmonics, suggesting that the cystic fibrosis case introduces a higher amount of nonlinear effects than the healthy case. From Figure 10 we observe that in asthma the BLA has higher values than in healthy, as well as higher variance of nonlinear contributions with about $10-15\,\mathrm{dB}$ (non-excited odd and even harmonics). Finally, the effects of smoking are also captured with the proposed method, showing a clear increase in the BLA values for smokers of about $5-10\,\mathrm{dB}$. The difference between smokers and non-smokers increases with decreasing frequency, which implies that valuable information can still be obtained at lower frequencies by reducing the influence of the breathing signal. This could possibly be achieved by applying special filtering techniques [15].

In short, our results suggest that interesting differences are present and can be further quantified to obtain novel indexes in classification studies. We speculate that these indexes may be helpful to understand the progress of the disease in the lungs. Furthermore, one may intuitively conclude that different pathologies alter the nominal morphology and structure of the lungs. From a physiological viewpoint, the non-homogeneity in the diseased lung structure leads to an asymmetric distribution of the air-flow in the airways, resulting in heterogeneous diffusion zones [14]. We expect that these will introduce various nonlinear effects, due to turbulent flow conditions and viscoelasticity (i.e. both nonlinear features of the lungs).

The measurements are disturbed by the non-stationary breathing signal, especially at the lower frequencies. This disturbance makes it difficult to interpret the results at lower frequencies. The most effective method to reduce this effect is to increase the measurement time. Unfortunately, this is not always practically feasible, e.g. a child with asthma has problems to undergo measurements longer than 30 seconds without significant fatigue caused by the resistance of the FOT-device.

V. Conclusions

In this paper we present a technique which allows detection and quantification of the nonlinear effects in the measurement instrumentation and the respiratory system by means of measuring the impedance. Based on this signal analysis, an optimization of the identification signal for the respiratory impedance has been proposed and applied successfully on healthy subjects and three respiratory alterations: asthma, cystic fibrosis and smoking.

It has also been shown that by replacing the excited frequencies of a multisine identification signal from even to odd frequency points, one can reduce the total variance on the measurement of the respiratory impedance by a factor three. Consequently, this gives a more reliable result for the respiratory impedance.

The method and theoretical development presented in this paper can be easily extended to other biological applications. Prospective developments include an improved prototype for low frequency excitation (i.e. closer to the breathing frequency) and advanced filtering techniques for non-stationary signals (breathing).

VI. Acknowledgments

The authors gratefully acknowledge the technical contributions of Niels van Nuffel and Mattias Deneut.

References

[1] Barnas, G.M. and Yoshino, K. and Loring H. and Mead, J *Impedance and relative displacements of relaxed chest wall up to 4 Hz*, J Appl Physiol, 62, 71-81, 1987.

[2] Birch, M. and MacLeod, D. and Levine, M. *An analogue instrument for the measurement of respiratory impedance uisng for the forced oscillation technique*, Phys Meas, 22, 323-339, 2001.

[3] Daroczy, B. and Hantos, Z. *An improved forced oscillatory estimation of respiratory impedance*, Int J Bio-med Comp, 13(3), 221-235, 1982.

[4] Daroczy, B. and Fabula, A. and Hantos, Z. *Use of noninteger-multiple pseudorandom excitation to minimize nonlinear effects on impedance estimation*, Eur Respir Rev, 1, 183-187, 1991.

[5] De Melo, P.L. and Werneck, M.M. and Giannella-Neto, A. *Effect of generator nonlinearities on respiratoy impedance*, Med Biol Eng Comp, 38(1), 102-108, 2000.

[6] Franken, H. and Clément, J. and Van de Woestijne, K.P. *Systematic and random errors in the determination of respiratory impedance by means of the forced oscillation technique: a theoretical study*, IEEE Trans Biomed Eng, 30(10), 642-651, 1983.

[7] Guyton, A. and Hall, J. *Textbook of medical physiology*, W.B. Sanders, 11th Edition, 2005.

[8] Ionescu, C. and De Keyser, R. *Novel parametric model for the human respiratory system*, Proc of the IASTED Int Conf on Modelling and Simulation, Palm Springs, USA, February 2003.

[9] Navajas, D. and Farré, R. and Rotger, M. and Peslin, R. *A new estimator to minimize the error due to breathing in the measurement of respiratory impedance*, IEEE Trans Biomed Eng, 35(12), 1001-1005, 1988.

[10] Navajas, D. and Farré, R. and Canet, J. and Rotger, M. and Sanchis, J. *Respiratory input impedance in anesthetized paralyzed patients*, J Appl Physiol, 69(4), 1372-1379, 1990.

[11] Oostveen, E. and Macleod, D. and Lorino, H. and Farré, R. and Hantos, Z. and Desager, K. and Marchal, F. *The forced oscillation technique in clinical practice: methodology, recommendations and future developments*, Eur Respir J, 22(6), 1026-1041, 2003.

[12] Schoukens, J. and Pintelon, R. *System identification. A frequency domain approach*, New Jersey: IEEE Press, 2001.

[13] Schoukens, J. and Pintelon, R. and Dobrowiecki, T. and Rolain, Y. *Identification of linear systems with nonlinear distorsions*, Automatica, 41(3), 491-504, 2005.

[14] Solway, J. and Fredberg, J. and Ingram, R. and Pedersen, O. and Drazen, J. *Interdependent regional lung emptying during forced expiration: a transistor model*, J. Appl. Physiol. 62(5), 2013-2025, 1987.

[15] Zivanovic, M. and Schoukens, J. *Time-variant harmonic signal modeling by using polynomial approximation and fully automated spectral analysis*, in Proc of the 17th European Signal Processing conference, Glasgow, UK, August 2009.